Linear Subarrays for Multi-Beam Satellites

Sangbae Oh*, Jungjin Shin*, Hyojoon Lim*, Joongki Park*, Heedong Do†, Namyoon Lee†
* C41 R&D Center, LIG Nex1, Yongin, Korea
† School of Electrical Engineering, Korea University, Seoul, Korea

***Abstract*—This paper considers hybrid array architectures with partially-connected analog networks for multi-beam satellites. It is shown that some subarray architectures, such as linear subarrays, can perform as well as fully digital implementation under certain circumstances. Not all subarray architectures, square subarrays for instance, exhibit such property. This observation highlights the importance of subarray architecture.**

I. Introduction

Facilitated by the recent technological advances, low earth orbit (LEO) satellite networks are now seen as a promising complement to the terrestrial counterparts. From the wide coverage it provides [1], it has a myriad of attractive use cases such as connectivity to rural areas, ships, aircrafts, and Internet-of-things.

Large communication range results in high signal attenuation, which naturally invites the use of high-gain phased array composed of hundreds of low-gain elements. Towards higher throughput and flexibility, multi-beam satellites has become popular [2]; for instance, OneWeb's satellites in the initial constellation utilizes 16 beams [3]. This multi-beam capability necessitates the use of multiple RF chains. Fully digital architectures can do the job, but with a requirement of one RF chain per array element. Given hundreds of array elements, fully digital implementation is not affordable for LEO satellites owing to their severe limitations on weight, size, and power consumption. As an alternative, the use of hybrid arrays are often considered. Specifically, partially-connected hybrid architectures comprising of multiple subarrays are considered owing to their cost-effectiveness compared to fully-connected counterparts [4].

From footprint considerations, uniform planar arrays (UPAs) are preferred for satellites. Being arranged in plane, a variety of subarray topology can be used (see [5, Fig. 6(a)]). For single user multiple-input multiple-output (MIMO) system, it is observed in [5, Fig. 7] that the best array topology goes hand in hand with a propagation characteristic. When it comes to multi-beam satellites, the performance would depend on the location of ground stations, which entirely determines the propagation channel in case of pure line-of-sight (LOS) propagation. A welcome news is that one can schedule ground stations to construct a channel favorable to the array architecture.

The present paper advocates the use of linear subarrays rather than more conventional square subarrays (see Fig. 1). It is shown that the hybrid arrays with linear subarrays can mimic the fully digital arrays when the ground stations are carefully scheduled.

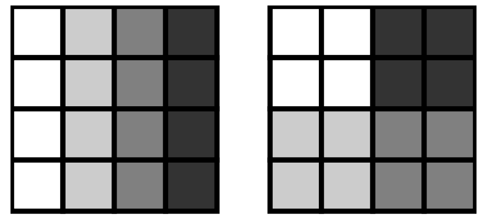

Fig. 1. Hybrid array architectures.

II. System Model

This section presents a system model that describes downlink transmission from the UPA-equipped satellite to K single-antenna ground stations. It is assumed that the bands allocated to the users do not overlap to avoid interference. Also, the total bandwidth is assumed to be much smaller than the carrier frequency.

A. Array Model

Consider a UPA-equipped satellite communicating with a single-antenna ground station. The UPA has dimensionality $N_x \times N_y$ and antenna spacings along the respective dimensions are d_x and d_y. For brevity, we adopt the zero-based numbering convention for all indices throughout the paper.

The coordinate system is chosen so that nth element ($n \in \{0, \dots, N-1\}$ with $N = N_x N_y$) locates at

$$\begin{bmatrix} x_n & y_n & 0 \end{bmatrix}^\top = \begin{bmatrix} d_x\left(n_x - \frac{N_x-1}{2}\right) & d_y\left(n_y - \frac{N_y-1}{2}\right) & 0 \end{bmatrix}^\top$$

where $n_x \in \{0, \dots, N_x - 1\}$ and $n_y \in \{0, \dots, N_y - 1\}$ are the quotient and remainder of n/N_y. The location of the kth ground station is

$$D_k \begin{bmatrix} \sin\phi_k \cos\theta_k & \sin\phi_k \sin\theta_k & \cos\phi_k \end{bmatrix}^\top \quad (1)$$

where D_k is the communication range, θ_k is the zenith angle, and ϕ_k is the azimuth angle. For convenience, let us introduce the notations $u_k = \sin\phi_k \cos\theta_k$ and $v_k = \sin\phi_k \sin\theta_k$, which is a widely used convention in phased array theory [6].

B. Channel Model

Consider a pure line-of-sight connection between the satellite and the kth ground station. Denoting the carrier frequency by f_c, the normalized channel vector $\boldsymbol{a}^*(\cdot)$ satisfies [6, Eq. 1.59]

$$[\boldsymbol{a}^*(u_k, v_k)]_n = \exp\left(j\frac{2\pi}{\lambda}(u_k x_n + v_k y_n)\right). \tag{2}$$

Such channel vector can be expressed as

$$\boldsymbol{a}^*(u_k, v_k) = \boldsymbol{a}_x^*(u_k) \otimes \boldsymbol{a}_y^*(v_k) \tag{3}$$

where

$$\boldsymbol{a}_x^*(u_k) = \exp\left(j\frac{2\pi}{\lambda}u_k x_n\right) \quad \boldsymbol{a}_y^*(v_k) = \exp\left(j\frac{2\pi}{\lambda}v_k y_n\right). \tag{4}$$

Here, $\otimes$ denotes the Kronecker product. The normalization constant can be incorporated into the signal-to-noise ratio, resulting in

$$\mathsf{SNR}_k = \frac{\lambda^2 G_t G_r P_k}{(4\pi D_k)^2 W_k N_0} \tag{5}$$

where G_t is transmit element gain, G_r is receive element gain, P_k is the radiated power for the kth ground station, W_k is the bandwidth allocated to the kth ground station, and N_0 is the noise spectral density.

C. Signal Model

Let us denote the analog and digital beamformers by $\boldsymbol{F} \in \mathbb{C}^{N \times N_{RF}}$ and $\boldsymbol{g}_k \in \mathbb{C}^{N_{RF}}$, respectively, where N_{RF} is the number of RF chains. The receive signal at the kth ground station can be described as

$$y_k = \boldsymbol{a}^*(u_k, v_k)\boldsymbol{F}\boldsymbol{g}_k s_k + v_k \tag{6}$$

where $s_k \sim \mathcal{N}_{\mathbb{C}}(0, \mathsf{SNR}_k)$ is the transmit signal and $v_k \sim \mathcal{N}_{\mathbb{C}}(0, 1)$ is the Gaussian noise. The power constraint is then

$$\|\boldsymbol{F}\boldsymbol{g}_k\|^2 = 1 \tag{7}$$

from

$$\mathbb{E}[\|\boldsymbol{F}\boldsymbol{g}_k s_k\|^2] = \|\boldsymbol{F}\boldsymbol{g}_k\|^2 \mathsf{SNR}_k. \tag{8}$$

III. Achieving Fully Digital Performance

As we consider partially-connected hybrid architectures, the analog network $\boldsymbol{F}$ has an additional constraint. Denoting the set of elements connected to mth RF chain by I_m, we have $[\boldsymbol{F}]_{n,m} = 0$ if $n \notin I_m$.

To attain a fully digital performance, we need to have

$$\|\boldsymbol{a}^*(u_k, v_k)\boldsymbol{F}\boldsymbol{g}_k\| = \sqrt{N} \tag{9}$$

for all k. With a given analog beamformer $\boldsymbol{F}$, the optimal digital beamformer is essentially the maximum ratio transmission

$$\boldsymbol{g}_k = \frac{\boldsymbol{F}^*\boldsymbol{a}(u_k, v_k)}{\|\boldsymbol{F}\boldsymbol{F}^*\boldsymbol{a}(u_k, v_k)\|} \tag{10}$$

where the normalization factor follows from the power constraint (7). Plugging (10) into (9), we obtain

$$\|\boldsymbol{F}^*\boldsymbol{a}(u_k, v_k)\|^2 = \sqrt{N}\|\boldsymbol{F}\boldsymbol{F}^*\boldsymbol{a}(u_k, v_k)\|. \tag{11}$$

We can rewrite it as

$$\begin{aligned}\boldsymbol{a}^*(u_k, v_k)&\boldsymbol{F}\boldsymbol{F}^*\boldsymbol{a}(u_k, v_k)\\ &= \|\boldsymbol{a}(u_k, v_k)\|\|\boldsymbol{F}\boldsymbol{F}^*\boldsymbol{a}(u_k, v_k)\|.\end{aligned} \tag{12}$$

Recalling the equality condition of Cauchy-Schwarz inequality, the equality holds if and only if

$$\boldsymbol{a}(u_k, v_k) \parallel \boldsymbol{F}\boldsymbol{F}^*\boldsymbol{a}(u_k, v_k) \tag{13}$$

for all k, where $\parallel$ denotes parallel symbol. Let us dissect it by observing mth subarray, i.e.,

$$\begin{aligned}&\underbrace{(\boldsymbol{a}(u_k, v_k))[I_m, \{0\}]}_{\substack{\text{Channel between } m\text{th subarray}\\ \text{and } k\text{th ground station}}}\\ &\parallel \underbrace{\boldsymbol{F}[I_m, \{m\}]}_{\substack{\text{Analog beamformer}\\ \text{for } m\text{th subarray}}} \underbrace{(\boldsymbol{F}[I_m, \{m\}])^*(\boldsymbol{a}(u_k, v_k))[I_m, \{0\}]}_{\text{Scalar}}.\end{aligned} \tag{14}$$

where $\boldsymbol{A}[X, Y]$ denotes the submatrix of entries in the rows of $\boldsymbol{A}$ indexed by set X and the columns indexed by Y, adopting the notation in [7]. This results in

$$(\boldsymbol{a}(u_k, v_k))[I_m, \{0\}] \parallel \boldsymbol{F}[I_m, \{m\}]. \tag{15}$$

Since it holds for all ground stations, for all k and k', we have

$$(\boldsymbol{a}(u_k, v_k))[I_m, \{0\}] \parallel (\boldsymbol{a}(u_k, v_k))[I_m, \{0\}]. \tag{16}$$

Put another way, for each m, the channels between mth subarray and K ground stations should be parallel.

One can easily check that the reverse direction also holds. If (16) holds, the choice

$$\boldsymbol{F}[I_m, \{m\}] = (\boldsymbol{a}(u_k, v_k))[I_m, \{0\}] \tag{17}$$

with any k satisfies (13). It is worth noting that there is no need for amplitude tapering at the analog side.

As per (16), if any subarray has two elements whose x-coordinates differ less than $\frac{\lambda}{2}$ and y-coordinates are identical, we have $u_0 = \ldots = u_{K-1}$ [8, Ex. 3.32]. Similarly, if any subarray has two elements whose x-coordinates are identical and y-coordinates differ less than $\frac{\lambda}{2}$, we have $v_0 = \ldots = v_{K-1}$. Therefore, hybrid architecture with square subarrays cannot perform as well as fully digital architecture unless all the ground stations are located at the same coordinate.

This severely strict condition can be relaxed by the use of linear subarrays with $N_{RF} = N_x$ in lieu of square one. From the condition above, only $v_0 = \ldots = v_{K-1}$ is required. In practical systems, this condition can be approximately satisfied by judicious scheduling.

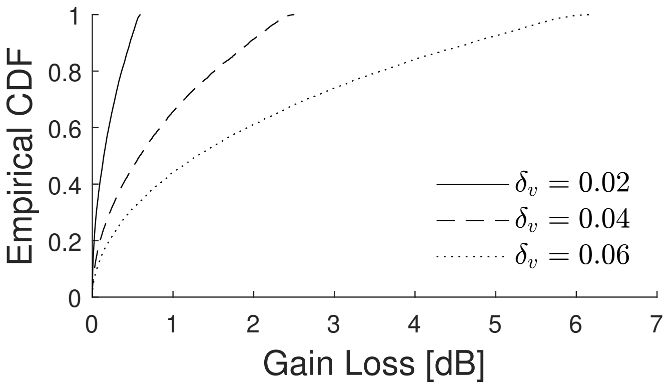

Fig. 2. Empirical CDF of the loss in gain.

IV. Simulation Results

In an actual operating environment, the performance of the hybrid arrays may fall short of that of the fully digital arrays because of the two assumptions we have made in the analysis:

- carrier frequencies of ground stations are identical
- v-coordinates of ground stations are identical.

The former condition is rather ideal since the fractional bandwidth of operating satellites is about 10% [3], ditto for the latter condition.

To see what happens when deviating from these assumptions, numerical study is conducted. The array parameters are set to $N_x = N_y = 20$ and $d_x = d_y = \lambda/2$. Eight ground stations, i.e., $K = 8$, are considered having coordinates

$$u_k \sim \mathsf{Uniform}(-1, 1) \qquad v_k \sim \mathsf{Uniform}(-\delta_v, +\delta_v). \tag{18}$$

The center frequency and bandwidth for each beam are set to 30 GHz and 150 MHz, respectively.

Fig. 2 depicts the empirical cumulative distribution function (CDF) of the loss in gain when the proposed hybrid architecture is used instead of fully digital one. That is,

$$\frac{\|\boldsymbol{a}^*(u_k, v_k)\boldsymbol{F}\boldsymbol{g}_k\|^2}{N}. \tag{19}$$

Ten thousands of random instances are generated for each δ_v. The simulation result demonstrates that the loss is less than 1 dB for $\delta_v = 0.02$. Note that the coverage area with $\delta_v = 0.02$ roughly corresponds to the belt of 22 km width.

V. Conclusion

This paper investigates a hybrid array architecture with linear subarrays. Its advantage over conventional square subarray is analyzed.

Some potential follow-up research directions are

- investigation of other array types
- extension to the case of aggressive frequency reuse where inter-beam interference exists
- joint optimization of scheduling
- consideration of multiple satellites.

References

[1] J. Park, J. Choi, and N. Lee, “A tractable approach to coverage analysis in downlink satellite networks,” *IEEE Trans. Wireless Commun.*, 2022.

[2] M. Á. Vázquez, A. Perez-Neira, D. Christopoulos, S. Chatzinotas, B. Ottersten, P.-D. Arapoglou, A. Ginesi, and G. Taricco, “Precoding in multibeam satellite communications: Present and future challenges,” *IEEE Wireless Commun.*, vol. 23, no. 6, pp. 88–95, 2016.

[3] N. Pachler, I. del Portillo, E. F. Crawley, and B. G. Cameron, “An updated comparison of four low earth orbit satellite constellation systems to provide global broadband,” in *IEEE Int’l Conf. Commun. Workshops*, 2021, pp. 1–7.

[4] S. Han, I. Chih-Lin, Z. Xu, and C. Rowell, “Large-scale antenna systems with hybrid analog and digital beamforming for millimeter wave 5G,” *IEEE Commun. Mag.*, vol. 53, no. 1, pp. 186–194, 2015.

[5] S. Park, A. Alkhateeb, and R. W. Heath, “Dynamic subarrays for hybrid precoding in wideband mmWave MIMO systems,” *IEEE Trans. Wireless Commun.*, vol. 16, no. 5, pp. 2907–2920, 2017.

[6] R. J. Mailloux, *Phased array antenna handbook*. Artech house, 2017.

[7] R. A. Horn and C. R. Johnson, *Matrix analysis*. Cambridge university press, 2012.

[8] R. W. Heath, Jr. and A. Lozano, *Foundations of MIMO Communication*. Cambridge University Press, 2018.